Dust extinction and intrinsic SEDs of carbon-rich stars

III. The Miras, CS, and SC stars[*,**,***]

A. Knapik, J. Bergeat, and B. Rutily

Centre de Recherche Astronomique de Lyon (UMR 5574 du CNRS), Observatoire de Lyon, 9 avenue Charles André,
F-69561 St-Genis-Laval cedex, France

Abstract. The present work is an extension of a recent study by Knapik & Bergeat (1997), and Bergeat et al. (1998b) henceforth called Papers I and II, respectively. The spectral energy distributions (SEDs) of about 440 carbon-rich stars and the interstellar extinction observed on their line of sights were analysed. The methods originally developed for Semi-Regular (SR) and Irregular (L) variables (Paper I: our groups CV1 to CV6) were then extended (Paper II) to the hot carbon (HC) stars (our groups HC0 to HC5) and related objects (RCB, BaII and HdC stars). Shortly, this is a kind of a pair method making use simultaneously of the whole SED from UV to IR.

Our approach is applied here to the galactic cool carbon-rich variables which were not considered in Paper I, namely the carbon Miras and very cool non-Miras, and the CS and SC variables. The carbon Miras with infrared silicate emission are also studied. The photometric CV1 to CV6 classification scheme of paper I is implemented, and we add here a later CV7-group and a specific SCV-group which corresponds to spectroscopic SC stars. A continuous S-SC-CS-C sequence is clearly supported by our results. The carbon stars with IR silicate emission included in our study do have carbon-rich SEDs of the three consecutive groups HC5, CV1 and CV2. They stand among the relatively hot carbon variables, in the 3600–3000 K range in effective temperature. The carbon Miras are satisfactorily described in this enlarged scheme. No specific extension is required since non-Miras are also found in the CV7 and SCV-groups. The derived group is however frequently phase-dependent in these large amplitude variables. Additional selective extinction of circumstellar (CS) origin is observed in variable amounts. The mean extinction law for the interstellar diffuse medium as tabulated by Mathis (1990) is shown to be relevant. It applies to both interstellar and circumstellar extinction with a possible CS neutral extinction in addition which would remain undetected here. The corresponding colour excess E(B-V) is larger at minimum light or intermediate phases than what it is at maximum light (where it can amount to zero). It is associated to large IR excesses attributed to the emission from CS dust. Long-term variations on thousands of days may be interpreted in terms of varying CS dust opacity on the line of sight. The dust influence is discussed. It is shown that scattering, if substantial on the line of sight in the observing lobe, has to be essentially wavelength-independent, i.e. due to large neutral scatterers, especially in high opacity objects like IRC +10216.

Finally, with the HC0 to HC5 classification of HC stars (Paper II), we obtain a fourteen groups sequence (HC0 to HC5 and then CV1 to CV7 from the earlier one to the latest one, and SCV for SC stars apart). The number of studied stars amounts now to about 600 that is about 40 stars per group on the average when the oxygen-type SEDs are subtracted. The effective temperature calibration of this classification scheme is currently in preparation.

Key words: stars: carbon – stars: circumstellar matter – stars: AGB and post-AGB – ISM: dust, extinction

1. Introduction

The first classification of the carbon-rich giants in discrete photometric groups was proposed by Knapik & Bergeat (1997, hereafter Paper I), and Bergeat et al. (1998b, hereafter Paper II). It is independent of any spectral classification. The methods were validated in Paper I for carbon variables through colour-colour and colour-galactic latitude diagrams. They provide for every documented star a CVi-group (intrinsic SEDs from i=1 the earliest one to i=6 the latest one in Paper I) and the amount of the interstellar extinction A_J in the J-filter. The colour excess is $E(B-V) \simeq 1.15A_J$ for the mean extinction law of the diffuse interstellar medium (Mathis 1990) which was shown to be relevant. A good agreement was obtained in most cases when those colour excesses were compared to field values from the maps found in the literature. No gap was actually observed and discrete CVi-groups are adopted here only for convenience. The main features of this new pair method, described in Sect. 2 hereafter, are

---

- the simultaneous use of the whole spectral range from UV to IR (up to 17 wavelengths with equal weights *a priori*),
- the derivation of the relevant CVi-group and selective extinction of dust through an accurate linear fit (see Figs. 1, 2, 4, 5, 6 and 7),
- $E(B-V) \simeq 0.02$–0.03 as a detection threshold,
- the derivation of a k-factor (Sect. 2.4), which should be a squared angular diameter on a relative scale (and not an angular diameter as erroneously stated in Sect. 6 of Paper I).

The quantity $k^{1/2}$ showed the correlation with true parallaxes (derived from the HIPPARCOS data: ESA 1997, henceforth called ESA) expected for stars populating a given range in linear diameters (see Fig. 3 and Sect. 6 of Knapik et al. 1998).

The study in Paper I was concentrated on carbon stars with small or moderate amplitudes of variations (namely Lb or SR variables) making use of the six CVi-groups. In Paper II it was extended to the HC stars (i.e. essentially the stars classified as early R on the grounds of their spectra) and related objects like HdC or BaII stars, and RCB variables. The RV Tau variable AC Her was also studied. Here we propose an extension of our pair method (see Sect. 2) to latter SEDs (cooler variables) with a CV7-group (Sect. 3) whose mean effective temperature amounts to nearly (2050 ± 200) K according to a preliminary calibration. It is then shown that the (spectroscopic) CS variable stars can be classified in the CVi framework of carbon stars, while an intrinsic SED denoted as SCV (for SC variables) is introduced to fit the (spectroscopic) SC variables (Sect. 4). A sequence S-SC-CS-C is indicated. The gap between SEDs seems to happen between spectroscopic SC and CS stars. A few carbon stars with IR silicate emission are studied in Sect. 5, as late HC or early CV stars. Finally, Miras are considered as such in Sect. 6 although no specific grouping is required. Variations of CV-group with phase are established for some documented variables of large amplitudes, while opacity variations predominate in other carbon Miras. The case of circumstellar (*CS*) extinction and emission is discussed whenever possible. Our method provides reliable results even for extreme objects like IRC +10216 (Sects. 6 and 7), which was not expected.

2. The analysis of extinction and the pair method

2.1. The classification scheme

The classification scheme of intrinsic (i.e. without selective dust extinction) SEDs is described in Sect. 3 of Paper I. It was derived from diagrams (colour-colour and galactic latitude *vs.* colour index). Provisional lists of reddened and presumably unreddened stars were thus made, which were slightly revised later on in the process. Then, intrinsic loci for unreddened stars were split into consistent boxes or groups in the colour-colour diagrams. The number of boxes was chosen so as to provide regular and significant intervals by taking into account the expected accuracies of observations and standard deviations on the mean values of colour indices. The classification scheme was achieved through a trial and error approach. No marked gap was observed which could have helped.

Finally, the mean intrinsic SEDs were thus established for the CV1 to CV6-groups (Sect. 3.3 in Paper I). Sixteen mean unreddened indices:

$$I_0(\lambda) = m_0(\lambda) - [1.08]_0 \tag{1}$$

and dispersions were calculated, $[1.08]_0$ and $m_0(\lambda)$ being the unreddened magnitudes at $\lambda = 1.08\,\mu$m (the reference wavelength) and at any used wavelengths. The former magnitudes were adapted from Baumert's (1972) data in a spectral band free of strong molecular features. The most remarkable feature is that the red-near infrared parts of the six SEDs nearly coincide while large differences are observed at shorter and longer wavelengths (see Fig. 3 in Paper I). The reader is referred to Sect. 2 of Paper II for the specific way in which the method was applied to the hot carbon stars (HC0 to HC5-groups).

2.2. The pair method

The method fully described in Sect. 4 of Paper I is then applied to the whole sample, including presumably unreddened stars as well. It makes use of the differences

$$y(\lambda) = m(\lambda) - I_0(\lambda) \tag{2}$$

between the observed magnitudes

$$m(\lambda) = m_0(\lambda) + A(J)r(\lambda) \tag{3}$$

and, for a given group tentatively considered, the mean unreddened indices $I_0(\lambda)$. If the latter are properly selected (i.e. if the appropriate CV-group is considered), a linear relation is thus expected between $y(\lambda)$ and the adopted extinction law $r(\lambda)$, the extinction $A(J)$ at $\lambda_J = 1.25\,\mu$m being the slope and $[1.08]_0 = m_0(\lambda) - I_0(\lambda)$ the intercept. Both quantities are simultaneously derived from the least square method. If the selected group and/or the adopted extinction law are wrong, the relation is no longer a linear one. The method is illustrated on the whole spectral range in Fig. 1 for C4121 = S Sct taken from Paper I: strong curvatures were observed when the indices of the group CV3 or CV5 were used instead of CV4 the right group for S Sct. Eqs. (2) and (3) should reduce to $y(\lambda) = [1.08]_0$ when there is no reddening: the observed points are then expected to scatter around an horizontal line (see Fig. 1 in Paper II). A computer code was thus written which studies the relation between $y(\lambda)$ and $r(\lambda)$ and the associated statistics as described in Sect. 2.3. At this stage, a few stars migrated from our "unreddened" list to the "slightly reddened" one and conversely.

2.3. The used statistics

Assuming a given group and extinction law were selected, the ordinate predicted is

$$y_p(\lambda) = A(J)r(\lambda) + <[1.08]_0> \tag{4}$$

where $A(J)$ and $<[1.08]_0>$ are the slope and intercept respectively, as deduced from the least squares method. The standard deviation on the slope σ_a is calculated from

$$\sigma_a^2 = \Sigma(y - y_p)^2 / (n-2)\,\Sigma(r - <r>)^2 \tag{5}$$

where $< r > = (\Sigma r)/n$, the reference to wavelength being omitted for clarity. The usual colour excess is for the diffuse law

$$E(B - V) = A(J)/0.873 \qquad (6)$$

The quality of the linear fit may also be estimated by making use of the standard correlation coefficient. The differences $Y(\lambda) = y(\lambda) - y_p(\lambda)$ were systematically analyzed for possible residual dependence on wavelength. Strong discrepancy of a given measurement may lead to reject it and start the analysis again.

Consistent discrepancies on a large wavelength interval need explanation. Most stars in this paper, especially carbon Miras, show strong IR excesses starting usually from the H or K-band, less frequently from the J or L-band. Those excesses are attributed to thermal emission from *CS* grains. The data points at shorter wavelengths can be fitted by a linear relation with good accuracy and increasing differences are then noticed in the IR (see e.g. Figs. 2, 5, 6 and 7). The extinction law of the diffuse interstellar medium taken from Mathis (1990) was successfully used as can be seen in the following sections and diagrams. The consequences and the interpretations we place on those diagrams are discussed hereafter, separately for each category of studied objects.

2.4. The k-factor

Once dereddening has been operated through Eq. (3), we should have ideally

$$m_0(\lambda) - I_0(\lambda) = < [1.08]_0 > = -2.5\log(k) \qquad (7)$$

at every wavelength but some scatter is of course observed. Thus we calculate the mean value $< k > = \Sigma k(\lambda)/n$ whose standard deviation is given by

$$\sigma_k^2 = \Sigma(k - < k >)^2/n(n - 1) \qquad (8)$$

It may be used as a signal to noise ratio for the whole method. The k-coefficient of Eq. (7) is the ratio of the dereddened star fluxes to those of a reference star of the same group (CV1 to 6) which would have the magnitude zero at $1.08\,\mu$m. Of course, the same ratio can directly be computed for unreddened stars. It will be confirmed that this is a squared angular diameter on a relative scale (Bergeat & Knapik, 1999). We emphasize here that the quantities $k^{1/2}$ already showed the correlation with true parallaxes as deduced from ESA, that are expected for stars populating a given range in linear diameters (see Fig. 3 and Sect. 6 of Knapik et al. 1998).

3. The CV7-group

3.1. A later intrinsic SED for carbon variables

In Paper I, we made use of the $CI_B = [0.78]-[1.08]$ colour index derived from Baumert's (1972) data. As quoted in Table 1 of Paper I, CI_B is nearly a constant (1.06 to 1.14) along the CV1 to CV6 sequence. This remarkable property was turned into advantage by using diagrams of e.g. CI_B *vs* ([1.08]-K)-CI_B (see
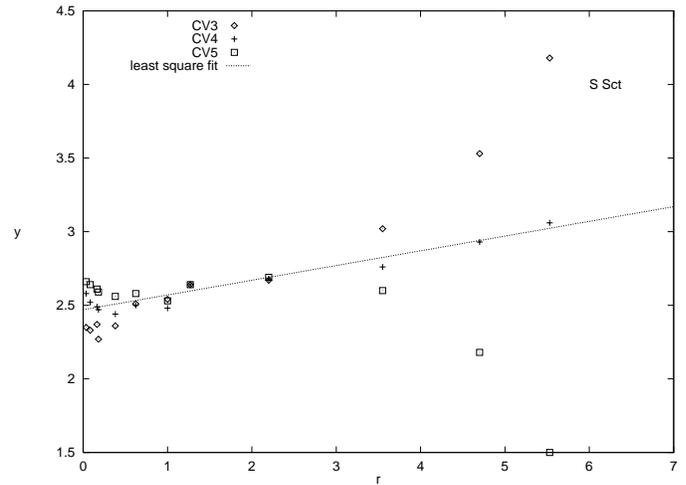

Fig. 1. The plot of the quantity y (λ) *vs.* r (λ) illustrating Eqs. (2), (3) and (4) in the case of C 4121 (S Sct). The abscissae are extinctions normalized at $1.25\,\mu$m. The ordinates are the colour excesses plus unreddened magnitude at $1.08\,\mu$m once a linear fit is obtained for a given box (here CV4). The intercept is thus $< [1.08]_0 >$ since the colour excess vanishes with extinction. The straight line was derived from the least square method (see text for details). Its slope is an evaluation of the extinction at $1.25\,\mu$m, namely 0.10 ± 0.01 (internal error).

Fig. 2 of Paper I): the reddening vector is nearly perpendicular to the intrinsic narrow locus of unreddened stars. Similar diagrams were used with the H, L or L'-magnitudes instead of the K-ones. They are slightly less efficient. While preparing the present analysis of carbon Miras, the authors found well-documented variables with SEDs notably redder than the CV6 one. Some of them were interpreted as reddened CV6 stars, making use of the above-mentioned kind of diagram. The interstellar extinction could not be responsible for many other SEDs (including some of high galactic latitude stars) as shown by the inspection of published maps (FitzGerald 1968, Neckel & Klare 1980, and Burstein & Heiles 1982). Those SEDs have to be intrinsically red (mean temperatures less than 2300 K) and/or to be affected by some *CS* reddening. This is the case of the Miras R For (C361), V CrB (C3682) and T Dra (C3921). Finally, we were able to add a seventh group (CV7) based on this limited sample of only three unreddened (negligible interstellar extinction) Miras at maximum light (except data in K, L etc.. of T Dra since IR excesses were obvious). This new group is documented and included in Tables 6 and 7.

3.2. The example of V393 Aur = AFGL 815

We present here the detailed results for V393 Aur (C 1050) which is quite typical of the CV7-group in every aspect. It was studied as an infrared object (AFGL 815 = IRC 40140 = IRAS 05440+4311) before being catalogued as the SRa variable V393 Aur (Kazarovets et al. 1993; formerly SVS 2629). The available magnitude ranges are 14.8–16.1 and 1.3–2.3 in the V- and L-filters, respectively. The short wavelengths data of Lockwood (1974) was especially useful. Infrared observations
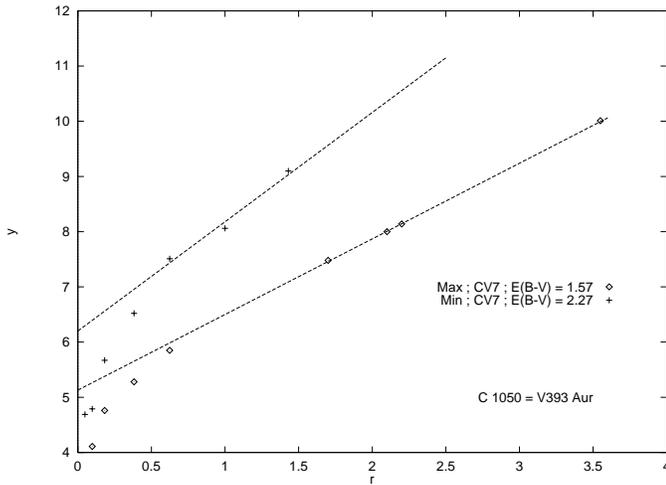
Fig. 2. The dereddening diagram for C1050=V393 Aur at two phases respectively close to maximum and minimum of the light curve. The corresponding regression lines are plotted. The slope is $A(J)$ the selective extinction at $\lambda = 1.25\,\mu$m and the intercept is $[1.08]_0$ the dereddened magnitude at $1.08\,\mu$m. Strong IR excesses relative to our solutions are observed for $r \leq 0.62$ (from the H-band and beyond) and for $r \leq 0.38$ (from the K-band and beyond) respectively. They are attributed to thermal emission from *CS* grains. See Sect. 2 for definitions and Sect. 3.2 for details.

Table 1. The cool reddened carbon variables of the CV7-group with C-entries from Stephenson (1989). A few stars not quoted in the GCVS (1985) are named with their IRAS-entry. The Miras are denoted by M. For $E(B-V) \leq 0.02$–0.03, the star is considered as unreddened. C496 is also CIT5 and C5358 is also CIT13. The E'(B-V) indices quoted are field values from published maps. Approximate phases and IR excesses (n = no excess or filter of first occurrence H, K, L, L', [12] or [25]) are found in the last column; (a) star at bright level; (b) = AFGL 1131: companion contribution subtracted; (c) = AFGL 971; (d) = AFGL 1235; (e) or 0.7 if beyond 2 kpc from sun.

C	name([M], l, b)	E_{B-V}	E'_{B-V}	Φ; Ex
189	NSV 438 (125.5 0.2)	0.53	0.5	min;H
361	R For[a] (M 215.8 -68.2)	0.00	0.00	0.0;n
361	R For[a] (M 215.8 -68.2)	0.28	0.00	0.6;H
496	V384 Per (M 148.2 -7.6)	0.63	0.6	0.0;K
572:	V414 Per (156.6 -10.9)	0.80	0.45	min;H
941	S Aur (173.5 -0.5)	0.27	0.24	0.5;K
	AFGL 799 (192.4 -8.8)	0.58	?	int;H
1050	V393 Aur (167.9 7.7)	1.57	0.90	max;H
1050	V393 Aur (167.9 7.7)	2.27	0.90	min;K
1322	V493 Aur (202.9 1.0)	1.49	0.60	?;n
1599	R Vol (M 284.2 -24.8)	0.26	0.18	0.3;K
1715	07240-1939 (234.4 -1.6)	0.16	0.15	?;n
1732	NSV3610[b] (234.5 -0.8)	0.56	0.5:	max;n
1732	NSV3610[b] (234.5 -0.8)	0.66	0.5:	int;n
1732	NSV3610[b] (234.5 -0.8)	0.50	0.5:	min;n
	V688Mon[c] (208.2 -1.7)	2.27	0.9	0.1;K
1907	V633 Mon (M 222.2 12.0)	0.07	0.08	max;K
2101	V346Pup[d] (M: 250.8 0.4)	2.33	0.2[e]	0.25;K
2334	UW Pyx (256.3 5.6)	0.28	0.26	?;n
2619	CW Leo (M 221.4 45.1)	2.34	0.00	0.16;H
2619	CW Leo (M 221.4 45.1)	3.67	0.00	0.27;H
3652	V CrB (M 65.4 51.2)	0.00	0.00	0.2;n
3748	16545-4214 (343.5 0.3)	1.86	0.7:	?;25
3921	T Dra (M 86.8 29.9)	0.00	0.03	0.0;K
4711	NSV 12861 (67.7 -2.2)	2.18	0.94	min;n
4939	V Cyg (M 86.5 3.8)	0.42	0.45	0.15;K
5358	V1426 Cyg (M 86.3 -9.4)	0.42	0.40	max;?
5358	V1426 Cyg (M 86.3 -9.4)	1.13	0.40	0.69;K
5358	V1426 Cyg (M 86.3 -9.4)	1.06	0.40	0.77;K
	LP And (M 108.5 -17.2)	2.09	0.15	max;L'

at various epochs were taken from Strecker & Ney (1974), Merrill & Stein (1976), Gosnell et al. (1979), Ney & Merrill (1980), Noguchi et al. (1981: values shifted as described in Sect. 2.3 of Paper I), and of course the IRAS-PSC data (1988; see Sect. 2.3 of paper I for the calibration used). The $y(\lambda)$ *vs.* $r(\lambda)$ dereddening diagram of V393 Aur is shown in Fig. 2 for selected data at two epochs (likely maximum at JD 2441659 and minimum light close to JD 2443472). The obtained solutions are CV7 for both epochs, with $E(B-V) \simeq 1.57$, $[1.08]_0 \simeq 5.13$ and $E(B-V) \simeq 2.27$, $[1.08]_0 \simeq 6.20$ respectively. The mean extinction law for the diffuse interstellar medium was again used as tabulated by Mathis (1990, Table 1). According to the available maps, $E(B-V) \leq 0.9$ is adopted for the interstellar medium on the line of sight. Our results support the existence of an additional variable selective *CS* extinction. The diagram appears as distorted at short wavelengths if a distinct selective law is adopted. We deduce selective *CS* contributions of $\Delta E(B-V) \gtrsim 0.67$ and 1.37 at maximum and minimum lights respectively. Neutral (i.e. independent of wavelength) extinction would however remain undetected from the present method. Lower limits of about $A_V = 2.4$ and 4.9 respectively, are thus deduced for the *CS* extinction at the above-mentioned epochs. Due to the thermal emission from *CS* grains which is not considered in our pair method, IR excesses appear in Fig. 2 when a comparison is made to the corresponding extrapolated straight line. The latter is a "model" of the reddened star in terms of a given intrinsic group and SED, affected by a given selective extinction $A(J)$, assuming a given extinction law is verified throughout. The excesses of V393 Aur start from the H-filter ($r=0.62$) at maximum light and from the K-filter ($r=0.38$) at

minimum light. Finally, we summarize the main features we found in common in many CV6 and CV7 stars:

- they are reddened distant objects not far from the galactic plane,
- they exhibit a strong *CS* extinction whose law, at the used wavelengths, seems close to the mean law tabulated for the interstellar diffuse medium, apart from a possible neutral component,
- the *CS* extinction varies with the phase of variations: $A(J)$ is usually minimum close to maximum light and conversely, maximum close to minimum light,
- the conspicuous IR excesses increase from the H or K-filter, and they can be attributed to thermal emission from *CS* grains.

Extinction variations on time scales larger than the stellar period are also observed (see Sect. 6). The reader is referred to Le Bertre (1992) and to Whitelock et al. (1997) who documented and studied a sample of carbon-rich variables on many cycles.

3.3. The results

Then we applied our pair method, as described in Sect. 2, to late carbon variables especially those whose analyses as reddened CV6 stars remained unsatisfactory. We were able to find 23 stars including 12 Miras (30 SEDs) which can be interpreted as CV7 stars reddened through the mean law for the diffuse medium as given by Mathis (1990). The results are quoted in Table 1. About 40 potential candidates were rejected because of missing data at short wavelengths. No E(B-V) excess substantially lower than the values read from maps is observed, but larger values are frequently found, especially at phases close to minimum light. The values at maximum light are smaller and eventually close to those (interstellar) from maps (see Table 1). As mentioned in Sect. 3.2, our analysis leads to a model of the observed SED (CVi-group) modified by some selective (interstellar + CS) dust extinction. This model is illustrated graphically by the straight lines and CVi-groups obtained (see Sect. 2.2). Thermal emission from CS grains is also observed resulting in substantial IR excesses relative to our model (see Figs. 2, 6 and 7 for CV7-stars). Part of the SEDs in Table 1 received the comment "n" in the last column, that is "no IR excess detected". This statement holds only for our wavelength range (up to IRAS [25]). We decided (see Paper I) not to include IRAS measurements at 60 μm and 100 μm since the 60 μm excess emission may often be due to contamination by galactic cirrus (Zuckerman 1993, Ivezic & Elitzur 1995). Intrinsic excesses contributing to detached shells are also observed in a sample of carbon stars (see Wallerstein & Knapp 1998 for a review) which belong to various CV-groups. The excesses in Table 1 presumably originate from hot dust in non-detached shells. Preliminary calibrations suggest effective temperatures in the 1850–2250 K range. Additional CS reddenings are thus more frequent in this low temperature group than they are in early CV-groups. It can easily be shown that the extinction law cannot be much different from the interstellar one we adopted. A non-selective (i.e. wavelength independent or neutral) contribution might also intervene however, which would remain undetected here. In those very cool atmospheres, CS grains are expected to condense close to the photospheric level (Salpeter 1977, Gail & Sedlmayr 1988), and the analyses of dust shells through Monte Carlo radiative transfer simulations lead to optical depths of the order of unity or larger (Lorenz-Martins & Lefèvre 1993, 1994).

3.4. Discussion

Part of Miras and large amplitude semi-regular variables (SRa-type) actually show a range in CV-groups according to the phase of the data. The earlier group is derived close to maximum light or just after it, the later one being observed close to minimum light. This is just what is expected along a temperature (and opacity) sequence, if temperature variations are predominant. Opacity variations in the atmosphere and CS envelope seem predominant in other cool, large amplitude variables where the variation range of the effective temperature is probably less than 300–400 K. This latter feature was already observed in a few CV6 Miras such as C833 = R Lep and becomes the rule in the CV7-group. Miras are studied as such in Sect. 6. It should be noted that the SEDs of the CV1 to CV6-groups were derived in Paper I on the basis of non-Miras only. The CV7-SED shows a distinctive break in the CV-sequence, with e.g. $\mathrm{CI_B} = 1.72$. The (presumably) fortuitous balancing probably responsible for the nearly constancy of the $\mathrm{CI_B} - \mathrm{index}$ along the CV1-CV6 sequence (see Table 6) no longer works. A severe change in line of sights opacities possibly occurs between CV6 and CV7. Dust contributions close to the photosphere may play a role. The generated extinction decreases for an expanding dust shell, the grains being pushed away by radiation pressure. However, it maintains large in the extreme objects described in Sect. 6. The picture may then be confused by dust backwarming on the atmosphere. It arises the question of validity of the intrinsic SED we adopted for CV7 since it relies on few stars. We consider however that it is globally correct since:

- no star with significant IR deficiencies was found so far,
- and in addition, several Miras like R Lep (CV6) or R For (CV7) display long-term variations superimposed on their usual light curve: negligible CS extinction is found while those stars reach maximum light at their bright level (see Sect. 6).

4. The CS and SC stars

4.1. Introduction

The stars of spectral type S are identified among cool giants by the bands of ZrO and LaO instead of the TiO-ones conspicuous in the spectra of the M-types stars. Their spectra also show strong enhancements of the s-process elements and a high C/O abundance ratio however less than unity (e.g. Keenan & Boeschaar 1980). The *intrinsic* S stars (e.g. Jorissen & Mayor 1992) are high luminosity AGB objects. Nucleosynthetised elements were recently brought to the surface by convective mixing. A piece of evidence is the observed technetium which has no isotope with period longer than 1 million years. It has often been argued that those stars might be a short-lived phenomenon between the stages of oxygen-rich and carbon-rich giants. The choice of the evolutionary sequence to be adopted is however controversial (Zuckerman & Maddalena 1989, de Jong 1989). A catalogue of galactic S stars has been published by Stephenson (1976).

4.2. The analysis of CS and SC stars

Stars like FU Ori or UY Cen show spectra intermediary between those of C and S stars. They are characterized by weak molecular bands, ZrO and CN being both present.

We selected 23 bright SC and CS stars, but only 21 stars in this sample proved sufficiently documented. Our pair method

Table 2. The CS stars in the present study. The stars C-entries from Stephenson (Stephenson 1989) are given. The Miras are referenced by (M) and the phase of the used observations is quoted. The number CN is the intensity index of the red system of the CN-bands in the near IR from Baumert (1972). Our solution is G, E(B-V) as quoted; (a) the group is HC5 (just earlier than CV1: see Paper II) at phase 0.9, but evolve to CVi at later phases.

C	name([M], Φ, l, b)	CN	G	E_{B-V}
136	W Cas (M 0.1 123.4 -4.3)	78	CV2	0.36
828	R Ori (M 0.8 191.7 -20.5)	72	HC5[a]	0.12
1561	R CMi (M 0.9 205.9 8.4)	68	HC5[a]	0.18
3367	TT Cen (M 0.6 306.4 1.9)		CV5	0.43
3665	RR Her (79.1 46.6)	68	CV2	0.00
4159	BD+103764 (43.3 2.3)	78	CV1	0.84
5570	RZ Peg (M 0.9 87.6 -17.8)	72	CV1	0.15

Table 3. The SC stars in the present study. The stars S-entries from Stephenson (Stephenson 1976) are given (S1093 is also C4152, V346 Aur is C797, and the IRAS-entries of S674 and S935 are given). Two possible Miras are referenced by (M:). The CN index is as in Table 2. Our solution is SCV for every star and E(B-V) as quoted.

S	name([M],Φ)	l	b	CN	E_{B-V}
117	GP Ori	186.0	-15.8	50	0.37
212	FU Mon	206.6	-4.9	45	0.26
244	V372 Mon	215.9	-4.3		0.24
556	U Vol	285.6	-17.0	47	0.04
674	10164-6044	285.4	-3.4	35	0.06
816	UY Cen	307.6	17.9	38	0.09
830	AM Cen	311.3	8.6	38	0.03
904	VY Aps	314.8	-16.1	30	0.11
935	16382-5727	330.2	-7.5	32	0.34
940	LQ Ara (M:, max)	328.2	-10.6	29	0.33
940	LQ Ara (M:, int)	328.2	-10.6	29	0.47
1093	VX Aql (M:, min)	32.5	-2.7	60	0.89
	V346 Aur	165.9	-3.5	64	0.31
	CY Cyg	85.5	1.7	38	0.14

(see Sect. 2) was again applied, but good solutions in terms of carbon CV-types could be obtained for only 7 stars (1 unreddened, 6 reddened: see Table 2) out of 20. Five of them are Miras. The extinction law is again the mean law adapted from Mathis (1990). There is evidence of CVi-variations with phase.

The SEDs of 6 of the remaining 13 stars (including UY Cen and AM Cen), presumably unreddened or slightly reddened, were found roughly similar to each other. We made a differential analysis of couples of stars. Our conclusion is that, within the errors, the 13 SEDs can be interpreted as a single intrinsic (unreddened) SED affected by interstellar extinction in various amounts. These stars are thus found as members of a homogeneous group we named SCV (see Table 3). The zero of the scale was then determined. As mentioned above, a few SCV stars are slightly reddened but finally, none of them was found unreddened in the present analysis (this is why SCV is not quoted in Table 7). This is a regrettable situation which will not change
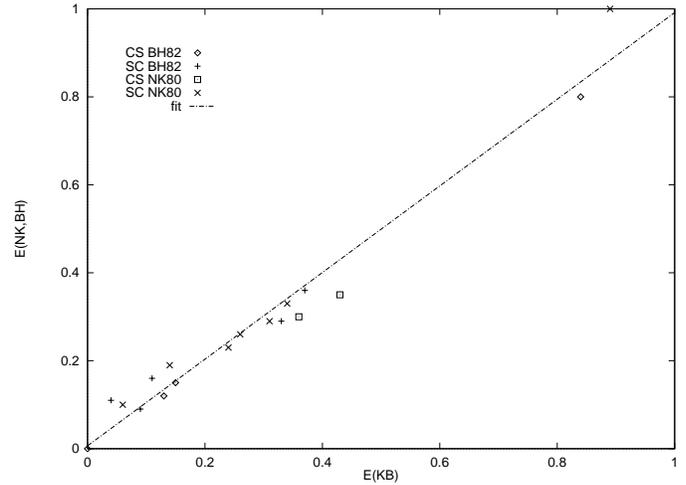

Fig. 3. A comparison of E(B-V) excesses from the maps and graphs of Neckel & Klare (1980, NK80) and Burstein & Heiles (1982, BH82) with values from the present paper (KB) for CS and SC stars. The regression line (9) is also shown.

since the brightest spectroscopic SC stars on the whole sky were studied here. It is worth noting however that AM Cen and U Vol are attributed small colour excesses (0.03 and 0.04 respectively).

4.3. The obtained extinctions

The results are given in Tables 2 and 3. The obtained reddenings were compared to the fields colour excesses E(B-V) taken from Neckel & Klare (1980), Burstein & Heiles (1982) and FitzGerald (1968). The corresponding diagram is shown in Fig. 3 for stars in common with the former two references, while the last one is not used since only ranges in colour excesses are provided. The linear fit shown in Fig. 3 is:

$$E_{NK-BH} = 0.985\,E_{KB} + 0.006 \tag{9}$$

with a correlation coefficient of 0.964. The standard deviation on the slope is 0.047, while 0.05 is found for a single ordinate estimate. The first bisector falls within the error domain in the diagram. This good agreement lends support to our approach, making use of the additional SCV-SED whose spectral shape differs markedly from the CVi-SEDs.

4.4. Discussion

Having completed the above analysis, we searched for independent arguments in favour of the grouping obtained in our study. First of all, Catchpole & Feast (1971) defined the SC stars as the ones closely similar in spectroscopic features to UY Cen the brightest member of this class. Out of our 13 SCV stars (Table 3), 10 at least belongs to their SC-class. They stated that those spectra are readily distinguished from the spectra of CS stars like R CMi, R Ori and W Cas (5 out of the 7 stars in Table 2 are classified as spectroscopic CS stars). The ZrO bands are absent or very weak in the latter stars, and CN much stronger than in the spectrum of UY Cen.

This feature is confirmed by the [CN]-index of Baumert (1972), an estimate of the intensity of the red system of the CN bands as observed in the red-near IR part of the spectrum. The values of the [CN]-index for the CS stars range from 68 to 78 in Table 2, which is very close to the 71–87 range of the mean values for the carbon variables which are classified as HC5, CV1 or CV2 stars (the range is 84–98 for CV3 to CV6 stars). The values quoted in Table 3 for the SC stars range from 29 to 64, the S stars displaying still lower values. Consequently, the stars in Table 2 can be found in the catalogue of carbon stars (Stephenson 1989) while only 2 stars in Table 3 are found in it, precisely those with the highest [CN]-values (64 for C797 = V346 Aur and 60 for C4152 = VX Aql). The transition between the CS and SC-classes probably falls in the 64–68 range of the [CN]-index. This is the transition between the SCV and carbon-rich SEDs. As can be seen in Tables 2 and 3, our CS stars are predominantly Miras (5 out of 7 stars) while our SC stars are predominantly semi-regular and irregular variables.

Finally, the remaining star (HD 121447, [CN]=26) is also classified as a BaII star (number 228 in Lü 1991). We found in our analysis the group to be K5g (i.e. an oxygen-type SED: see Bergeat & Knapik 1997) with E(B-V)=0.05; According to Jorissen et al. (1985), this is the coolest barium star, and this spectroscopic binary with $P_{orb} = 185\overset{d}{.}7$ might be an elliptical variable: IT Vir with V=7.82–7.86 in the 73rd name-list of variable stars (Kazarovets & Samus 1997).

According to Catchpole & Feast (1971), both classes could be closely related and possibly indicate the existence of a continuous sequence between the C and S giants. Our analysis proves that the CS and SC stars should be distinguished. The former stars exhibit SEDs close to those of carbon variables (CV) while the latter ones display a SED intermediary between those of C and S stars we name SCV. Its colour indices explore the same ranges as the CV-stars but the resulting SED is markedly different from any of the CVi-distributions. Thus we are unable at present to propose an estimate of the corresponding effective temperatures.

An additional remarkable feature is the following: we found no IR excess relative to the SCV-solution, starting from the filter H, K or L.., in the diagrams of the SCV stars. Weak or absent IR excesses are thus indicated in SCV stars, except possibly in the far IR. Such excesses are eventually observed with respect to CV-solutions in the diagrams of CS stars as it is the case for normal C stars. They are attributed to thermal emission from *CS* carbonaceous grains. Our CS stars are predominantly Miras while the SCV stars are usually non-Miras.

5. The carbon stars with IR silicate emission

5.1. Introduction

There are a few carbon stars whose low resolution IRAS spectra (LRS; IRAS Science Team 1986) do exhibit the characteristic signature of silicates at $10\,\mu m$ and eventually $18\,\mu m$ (Little-Marenin 1986, Willems & de Jong 1986 and Benson & Little-Marenin 1987). Two models have been proposed:

Table 4. The stars with IR silicate emission. The C-entries from Stephenson (1989) are given and/or a variable name from the GCVS. Our solution is the group G and the colour excess E(B-V) while E'(B-V) is the field value from the literature. Also given the excesses at IRAS wavelengths. Finally, W Cas may not be an IR silicate carbon star; (a) entry 1633 in Stephenson (1973) the first edition of the catalogue of cool carbon stars.

C	name	G	E_{B-V}	E'_{B-V}	E_{12}	E_{25}
136	W Cas	CV2	0.36	0.30	0.01	0.08
1653	BM Gem	CV1	0.15	0.14	2.2	2.7
2011		CV2	0.37	0.40	4.4	5.4
	V496Car[a]	M6g	0.14	0.13	0.5	0.5
4595	HD 189605	HC5	0.16	0.15	2.9	3.9
4923	V778 Cyg	CV1	0.30	0.33	2.6	3.2
5948	EU And	CV2	0.25	0.24	1.6	2.3
	AC Her	G0g	0.17	0.20	6.3	8.1

– a binary system, the silicate shell having been produced by an oxygen-rich giant (possibly obscured) not observed yet,
– an only giant whose atmospheric composition recently switched from oxygen-rich to carbon-rich (third thermal pulse in TP-AGB models; e.g. Straniero et al. 1997 and references therein).

Skinner et al. (1990) however argue that M stars with SiC dust, C stars with IR silicate dust signature, and S stars with either grains, are all objects whose photospheric C/O abundance ratio is close to unity, the type of dust which condenses being unpredictable. We note that the SC and CS stars studied in Sect. 4 are involved as well.

5.2. Our analysis

We have collected in Table 4, the results for 7 carbon stars (or formerly classified so) with silicate infrared emission. We compare them to AC Her, the RV Tau star which also displays those signatures. Its detailed analysis was presented in Paper II. We have included C136 = W Cas, a CS Mira (studied in Sect. 3), whose LRS spectrum was commented as "noisy silicate emission" by Chan (1994). Except for AC Her, the only oxygen-type SED found here is M6g for V496 Car which had the entry 1633 in the 1973 edition of the General Catalogue of Cool Carbon Stars (Stephenson 1973) and was then rejected from the next edition on the grounds of a M5 III spectrum observed by N. Houk (Stephenson 1989, Table 2). Skinner et al. (1990) suggest that it may be an S star. The other six stars are classified as HC5, CV1 or CV2, that is late HC or early CV stars.

There is thus no doubt that their SEDs show the signatures of carbon stars. From preliminary calibrations, the corresponding range in effective temperatures should be 3600–3000 K at most. It would be interesting to enlarge the studied sample and check whether they all fall in this narrow range in our classification. Our values of the E(B-V) colour index are remarkably close to the E'(B-V) values from maps in the literature (see Table 4). Practically, no room is left for a selective circumstellar

extinction. A *CS* emission is however present. In order to document the case, the extra-emission in the IRAS [12] and [25]-bands are quoted in Table 4, as deduced from the extrapolation of our model (group and colour excesses). The corresponding entries of W Cas are found negligible. The colour corrections were applied to the IRAS photometry and the [12]=1.5 value we obtained is consistent with the LRS spectrum re-processed by Chan (1994). The classification of this CS Mira as an IR silicate emission star is thus very questionable, and we do not consider it further. The other IRAS excesses range from about 0.5 mag. in V496 Cyg to 8.1 mag. in AC Her, with no large gap left. The large values quoted for AC Her are probably due to the marked temperature contrast between the star (group G0g, that is about 6000 K) and the dust (say less than 1800 K). The much cooler carbon star C2011 which has very large excesses at $12\,\mu$m and $18\,\mu$m, also shows substantial excesses in H, K and L quite similar to those of AC Her. The other stars with lower IRAS excesses show possible weak excesses or no excess at all at shorter wavelengths. The magnitude of near IR excesses are thus positively correlated with the intensity of their IR silicate features.

5.3. Discussion

The present data is not sufficient to settle a definitive conclusion. The silicate-rich envelopes seem directly associated to the observed stars, with no binarity required. The Mira W Cas which has no appreciable excess should be rejected from the sample. The RV Tau-type star AC Her is quoted only for comparison in Table 4. The data in Table 4 are consistent with the suggestion of Skinner et al. (1990) on unpredictability of dust type at $C/0 \simeq 1$. It arises the question whether "dirty" or "astronomical" silicates, as invoked to model the SEDs of extreme oxygen-rich cool giants (e.g. Jones & Merrill 1976, Rowan-Robinson & Harris 1982, Lefèvre et al. 1982), may explain those near IR excesses. Except in the UV, the complex part of the index of refraction is negligible for terrestrial silicates shortward of $7.5\,\mu$m (e.g. Pollack et al. 1973). Therefore, the complex refractive index is set to a large value (say 0.1) if dirty silicates are considered, while ad hoc wavelength-dependent values (however acceptable) are adopted for astronomical silicates. Preliminary Monte Carlo simulations of radiative transfer in spherical symmetry (such as those of Lefèvre et al. 1982) for two prescribed dust components (such as in Lorenz-Martins & Lefèvre 1994) favour carbonaceous grains as an explanation for the IR excesses which are not necessarily located at the same place as the silicate grains. Such a study is however hampered by the fact that the true spatial distribution of the dust is unknown at present. The other main conclusion is the interstellar origin of the selective extinction observed. To power the strong silicate dust signature observed in the IR, a substantial absorption increasing in the UV is expected from $0.3\,\mu$m or eventually $0.4\,\mu$m for basalt (Lamy 1978), if a sufficient number of silicate grains are seen on the line of sight to the star. The U-observations of our stars show no obvious deficiency relatively to our solution (essentially AC Her and C2011 which are well-documented and exhibit strong IRAS

excesses). The data at hand is however insufficient to warrant UV silicate absorption is absent. Simultaneous spectrophotometric UV observations down to $0.15\,\mu$m at least, should be secured and compared to our (extended) solutions. The *CS* extinction whose absorption part powers the excesses has to be:

- essentially independent of wavelength at least up to $\lambda_J = 1.25\,\mu$m which points to large grains (radii $a \simeq 0.3\,\mu$m or even larger),
- and/or strongly non-spherical in distribution (e.g. a disk or torus seen at a large inclination angle, nearly pole-on), or even patchy (blobs formation).

We reached similar conclusions in Paper II for HD 100764, AC Her and a sample of RCB-variables at maximum light.

6. The carbon Miras

6.1. The pair method applied to carbon-rich Miras

The carbon-rich Miras were not included in Paper I due to their large amplitudes of variation. Miras (especially oxygen-rich ones) are known to exhibit light curves which do not repeat faithfully from one cycle to the other (Lockwood & Wing 1971, Lockwood 1972). Notes in the General Catalogue of Variable Stars (Kholopov et al. 1985, henceforth called GCVS, and extensions published in the Information Bulletin on Variable Stars 1985 to 1997) contain frequently mean maximum values, while the range of extreme maximum and minimum are quoted in the main table. The SEDs of Paper I were more easily defined from small amplitude variables. Semi-regulars with relatively large amplitudes (SRa) were however included and sets of nearly simultaneous multicolour photometry selected whenever possible. There was some evidence that the photometric group of those stars may change with phase. The effect is still more pronounced in the case of many Miras. The results now available from the data at hand are given for 73 carbon Miras in Table 5 (only available in electronic form at the CDS). Unfortunately, sufficient multicolour measurements at various phases are available for only a limited sample of Miras. Seventy-five entries can be found in the first part of Table 5, each of them corresponding to an analysed SED. Fifty-six carbon Miras have thus been studied with a solution found (group and E(B-V) determined at least at one phase). Uncertain and incomplete results are reported for 17 additional Miras (and 17 SEDs) in the second part of Table 5. They are considered as very provisional but may be of some help. We had frequently to collect data secured during different cycles at phases within a given range like 0.05–0.15 or 0.3–0.5 for instance, and attribute the obtained SED to phases 0.1 or 0.4 respectively. This is of course a poor substitute for simultaneous multicolour photometry, and poorer meaning and lower accuracy necessarily result. The elements were usually taken from the GCVS and its extensions. The elements from HIPPARCOS (ESA 1997, vol. 11) were also considered. They give phases consistent with those from GCVS, at least roughly, with the exception of C828 = R Ori for which we adopted the HIPPARCOS values JD 2448673.5 + $379\overset{d}{.}0$ (ESA).
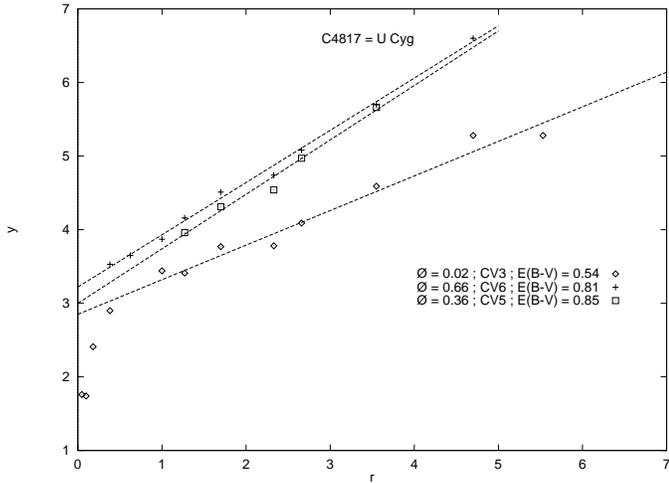
Fig. 4. Same as Fig. 2 for C4817 = U Cyg at three phases: maximum light and two intermediary phases with corresponding regression lines plotted. Infrared excesses due to thermal emission from *CS* grains are noted for $r \leq 0.62$ (from the H-filter and beyond). See text for details.

As expected, the redder the SED, the later the obtained photometric group. The earliest group is thus obtained at phases close to maximum light or slightly after (typically phases 0.00–0.15) and a later one is usually observed at phases close to minimum light (0.4–0.6). Effective temperature variations and opacity effects during pulsation cycles are coupled with angular diameter variations. There is a relatively well-defined relation between the effective temperatures and our CV-classification (Bergeat & Knapik 1999). An extensive study should be based on a larger body of data and this is what we are planning to do in the near future. For the time being, we present a few cases of carbon Miras (U Cyg, R Lep, V1426 Cyg = CIT13 and CW Leo = IRC+10216) we found sufficiently documented for our purposes.

6.2. The carbon Mira U Cyg

In most cases, the colour excess found at intermediary or late phases is larger than its counterpart at early phases close to maximum. Sometimes the difference between colour excesses deduced at various phases is not significant. This is not the case of the Mira C4817 = U Cyg. The $y(\lambda)$ *vs.* $y(\lambda)$ diagram at three phases are plotted in Fig. 4 (CV3 and E(B-V)=0.54 at $\Phi = 0.02$, CV5 and E(B-V)=0.85 at $\Phi = 0.36$, and CV6 and E(B-V)=0.81 at $\Phi = 0.66$). Unfortunately, no IR data was available at $\Phi = 0.36$ and the corresponding (CV5) solution should be attributed a lower weight. The star is seen in a strongly reddened field and E(B-V)=0.2 to 0.9 is expected from the maps in FitzGerald (1968), if its assumed distance lies between 0.5 and 1.0 kpc, a reasonable range from HIPPARCOS data (HIP 100219A, ESA). It is located just outside Zone 299 of Neckel & Klare (1980) where E(B-V) increases steeply from 0.4 at 400 pc to 0.75 at 600 pc. We found a slightly smaller colour excess (0.42) for V Cyg, a carbon Mira located in the same field (0.4–0.6 kpc). Finally, we consider the above value at maximum

(i.e. 0.54) as representative of the interstellar extinction on the line of sight, and attribute the additional 0.3 excess at intermediary phases to *CS* grains. The star U Cyg is representative of carbon Miras with large changes in CV-group. These ranges are experienced during every cycle and we interpret them in terms of large amplitudes in effective temperature (possibly 600 K for U Cyg, e.g. 2300–2900 K).

6.3. The cool end of the sequence

Colour excesses substantially larger than the expected interstellar value are frequently noticed for the coolest (CV5 to CV7) Miras even at phases close to maximum light (see Sect. 3 and Table 1). If *CS* grains are truly responsible of the additional extinction inferred, this is exactly what to expect. Concurrently, we have searched for pieces of evidence of a cooler intrinsic SED (say CV8), but we were unable to document such a group. More precisely, we failed to detect high galactic latitude stars with consistent SEDs substantially redder than the one adopted for CV7. In addition, no low galactic latitude star was found with accurate interstellar extinction from maps, whose dereddening could lead to a SED redder than CV7. If confirmed, this would imply that the coolest carbon variables have effective temperatures of nearly (2050 ± 200) K. The much lower temperatures sometimes quoted, would then be due to strong *CS* opacity effects, the direct stellar photons observed being too few. Consequently, the seven groups (CV1 to CV7) previously defined prove a sufficient framework for Miras analyses, at least on the basis of the presently available data.

6.4. The nearby Mira C833 = R Lep

The coolest objects with large amplitudes of variations are classified as CV6 or CV7 stars. They radiate a large part of their energy in the IR range. They often display the same CV-group upon a large phase interval or even upon several cycles, for thousands of days. Variations of effective temperature less than 300 K are thus indicated along such time intervals. Some of those stars also exhibit long term variations like R For or R Lep (e.g. Whitelock et al. 1997). We present now a study of C833 = R Lep, a nearby cool carbon Mira which was recently faint on several cycles ($JD \simeq 2449700$ and later). The HIPPARCOS elements ($JD2448620.24 + 444^d.0$) yield a good phase fit to the recent observations. Our main analysis deals with previous "bright" cycles. The group was CV6 with varied selective extinctions derived. Its HIPPARCOS observed parallax is (3.18 ± 0.76) mas (ESA) which would make it an underluminous star.

HIPPARCOS measurements are however affected by biases (Knapik et al. 1998), especially the Lutz-Kelker bias. Knapik et al. studied the space distribution of carbon giant stars from HIPPARCOS data and calculated the true parallaxes of an unbiased sample made of the same stars. The estimate of true parallax we obtained for R Lep is 2.97 mas only, which would imply $< M_K > = -7.7$, in the locus of carbon variables of the PL-relation of Bergeat et al. (1998a, their Fig. 1a), slightly

above its lower edge. According to this result, R Lep is not markedly underluminous, but this is of course a statistical argument, and the only way to make sure is a new and more accurate parallax measurement. According to published maps, this nearby star (300 pc) should be affected by a negligible interstellar extinction. As shown by the $y(\lambda)$ *vs.* $y(\lambda)$ diagram (Fig. 5), $E(B-V) \simeq 0.02$ is observed at maximum light, and $E(B-V) \simeq 0.6$ at $\Phi \simeq 0.38$. The additional 0.58 mag. can be attributed to *CS* dust. From the near IR (JHKL) photometry of Whitelock et al. (1997) and visual magnitudes from AAVSO (Mattei 1997), we anticipate for those faint cycles of R Lep the same group CV6 with $E(B-V) \simeq 0.4 \, \text{to} \, 1.3$ near maximas and minimas respectively. The increase of the colour excesses relative to the "bright" cycles, ranges from 0.4 at maximum light to 0.7 at minimum light. An additional 0.6–1.4 mag. dimming of the dereddened $[1.08]_0$ is observed which could be due to a contribution of large neutral carbonaceous grains. Unfortunately, this latter result is unconfirmed since we are missing simultaneous multicolour photometry in the visible. The visual light curve published by Mattei show a possibly similar event around JD 2436000. This interpretation would imply additional selective and neutral extinctions occurring on the line of sight in dense puffs, with no important change in the star properties (CV6). The star then returns to the normal "bright" level by "dust clearing", the grains leaving the line of sight and/or decreasing strongly in density by dilution during expansion and/or destructive collisions. We have already discussed the occurrence of such dense puffs in the vicinity of RCB-variables (see Paper II). Additional data is however needed before a firmer conclusion can be reached.

6.5. The CV7 Mira C5348 = V1426 Cyg = CIT13

Other cases with appreciable contributions of the interstellar and *CS* reddenings on a very cool intrinsic SED (presumably CV7) are more difficult to deal with. This is the case of C5348 = V1426 Cyg = CIT13 which appears as a CV7 star irrespective of the phase of the observations used (see Fig. 6). The colour excess found close to maximum light ($\Phi \simeq 0.15$) is 0.42 which is close to the 0.4 field value estimated from published maps. Two analyses with nearly simultaneous data could be made at $\Phi \simeq 0.69$ and 0.77 respectively. The slight difference between those excesses is not significant and the additional 0.7 mag. on E(B-V) can be attributed to the *CS* reddening. The objects like CIT13 are intermediary between the cool optical Miras, e.g. R Lep (CV6) and R For (CV7), and the extreme objects like CW Leo = IRC+10216 (also a CV7 star: see next subsection).

6.6. The extreme object C2619 = CW Leo = IRC+10216

The object CW Leo is an extreme cool dust-enshrouded carbon star whose extended shell and detailed chemistry deserved many studies (see Glasgold 1996 for a review and more recently Doty & Leung 1998). Other galactic objects belong to the same category like LL Peg = AFGL3068 an even more obscured carbon Mira (Sopka et al. 1985, Le Bertre et al. 1995 and Winters
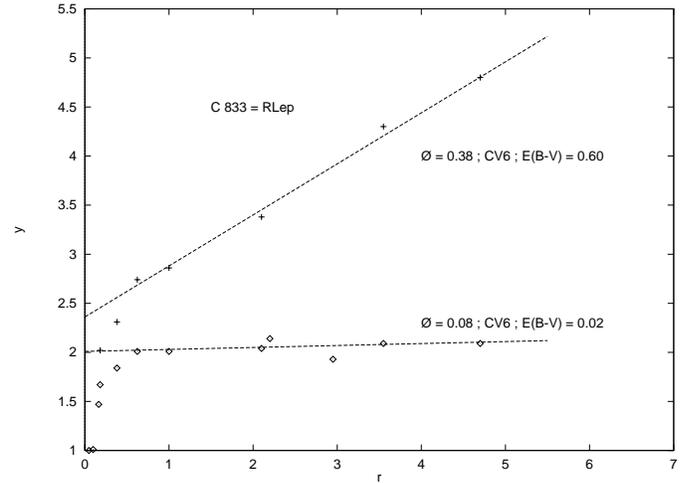
Fig. 5. Same as Fig. 2 for C833 = R Lep (during bright cycles) at two phases close to maximum and minimum respectively. The small reddening at maximum light is attributed to interstellar extinction on the line of sight. The corresponding regression lines are plotted. Infrared excesses due to thermal emission from *CS* grains are noted for $r \leq 0.38$ (from the K-filter and beyond). See text for details.
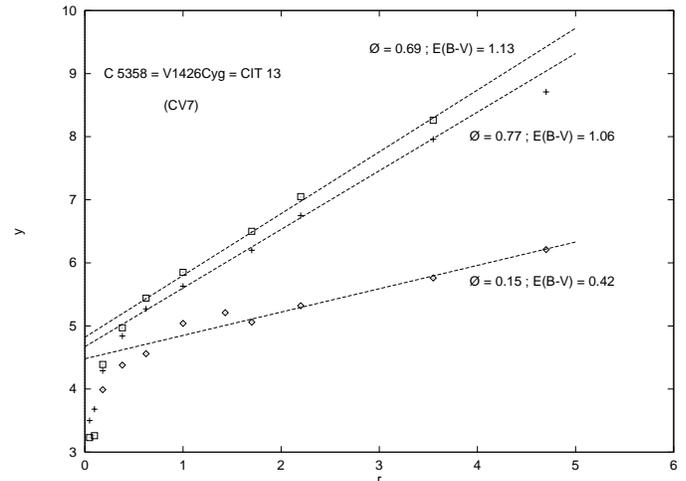
Fig. 6. Same as Fig. 2 for C5348 = V1426 Cyg = CIT13 at three phases (maximum and intermediary phases respectively). The reddening at maximum light (during bright cycles) at two phases close to maximum and minimum respectively. The small reddening at maximum light is attributed to interstellar extinction on the line of sight. The corresponding regression lines are plotted. Infrared excesses due to thermal emission from *CS* grains are noted for $r \leq 0.38$ (from the K-filter and beyond). See text for details.

et al. 1997) with a period of 700 d. CW Leo is classified as a Mira variable of period 630 d in the GCVS. It was unfortunately too faint for HIPPARCOS observation but this is a nearby object (100–250 pc from sun is usually adopted; e.g. Bergeat et al. 1978). A negligible interstellar extinction is thus expected from maps in the literature, which is a favourable circumstance.

The published photometric observations of CW Leo are less numerous that might be anticipated from the large number of references found in the SIMBAD database at CDS. In addition,
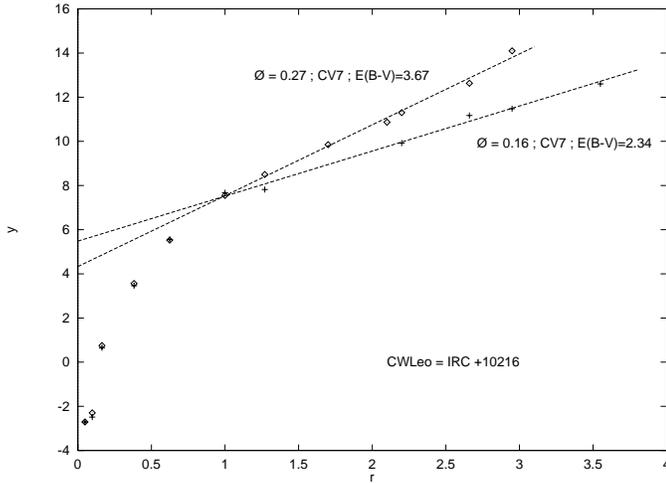
Fig. 7. Same as Fig. 2 for C2619 = CW Leo = IRC+10216 at two phases. No appreciable contribution from interstellar extinction is expected on the line of sight. The regression lines corresponding to the two solutions CV7 with E(B-V)=3.67 and 2.34 respectively, are shown. Infrared excesses due to thermal emission of *CS* grains are noted for $r \leq 0.62$ (from the H-filter and beyond). See text for details.
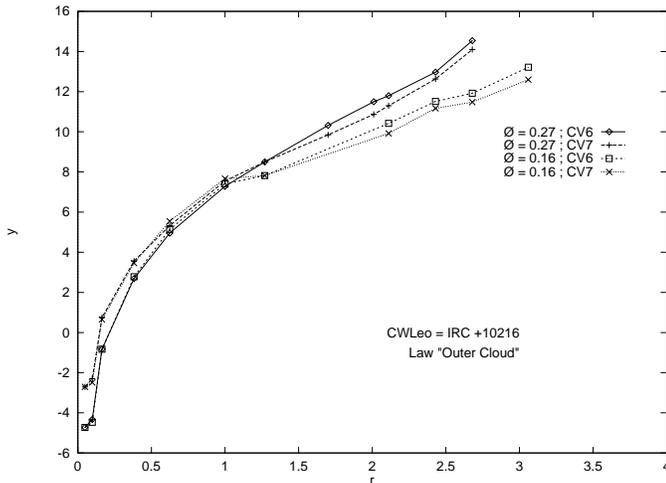

Fig. 8. Same data as Fig. 7 (CW Leo = IRC+10216) for CV6 and CV7 with the "outer cloud" extinction law of Mathis (1990). No linear fits can be accepted on those curved plots for $r \leq 1.0$, which means this law is not suitable here.

we need nearly simultaneous multicolour photometry from UV to IR since the ranges of variations are large even in the IR. Here, we apply our method to the short wavelengths 0.6 to $0.91 \, \mu m$ data and IR observations of Le Bertre (1988) near JD 2446918, and another SED near JD 2446225 making use, in addition, of Alksnis (1989) and Le Bertre (1987, see also 1992). The former SED at phase 0.27 is the best defined since all the data is nearly simultaneous. The later one at a phase of roughly 0.16 is in fact a "composite" since compatible observations at the same phase from other cycles were added at some wavelengths. The level of confidence is thus lower, but we wished to explore a SED closer to maximum light. We were convinced *a priori* that our method which makes use of the direct (transmitted as op-

posite to scattered) photons would not work here, due to large *CS* opacities and presumably, substantial multiple scattering. The y (λ) *vs.* y (λ) diagram of Fig. 7 displays the satisfactory (surprisingly enough) solutions CV7 with the large extinctions $E (B - V) \simeq 3.7$ and 2.4 respectively, which are entirely local to the source. The colour excess of 3.7 is the largest one we derived so far for a carbon star. If this analysis is correct, the effective temperature of the central object should be in the 1900–2200 K range found from the CV7 stars with measured angular diameters (Bergeat & Knapik 1999). An IR excess increasing from r=0.62 (H-filter and beyond) is noted with little difference between our two epochs as shown also by the light curves of Le Bertre (1992). This is the thermal emission from *CS* dust located in a very extended region. We must emphasize that any neutral extinction on the line of sight would remain undetected here. If effectively present, it prevents us from subtracting the net flux derived from the extrapolated regression lines in order to disentangle the *CS* emission. Light scattered in the observing lobe may also intervene and this point is discussed hereafter in Sect. 6.7.

We have also tested the influence of the adopted extinction law. To this purpose the "outer cloud" law of Mathis (1990) was used instead of the mean law for the diffuse medium he quoted (see his Table 1). The "outer cloud" law is less selective in the visible than the law for the diffuse medium we used successfully. It can be modeled by introducing larger grains in increased proportions. No reasonable fit for any CV-group could be obtained here. To illustrate the point, the diagram for the groups CV6 and CV7 and the "outer cloud" law is shown in Fig. 8. Appreciable curvatures can be seen on the entire spectral domain. It does not mean that any other combination of a CV-SED and special extinction law is ruled out, but that the agreement observed in Fig. 7 is the best obtained so far and needs to be explained. The statement that can be made is that *the selective part of the large extinction found follows a law which is close to the mean law for the diffuse interstellar medium, at least at two phases and for wavelengths shorter than* $1.65 \, \mu m$. From this point, constraints result on the fraction of light scattered in the instrumental observing lobe. If wavelength dependent, it has to be small (negligible here means less than 10-20% of the total light). Substantial scattering is however required by transfer models to explain the extensions of CW Leo images in the visible and the *CS* polarization at the K-band (e.g. Groenewegen 1997). The remaining possibilities are neutral scattering by large grains or a scattered contribution proportional to the transmitted light. Concerning the latter case, scattered photons reaching the observer through such a thick "dust atmosphere", come from the external layers where the scattering cross section affects light transmitted by the deeper layers (we derived total optical depths in excess of 6 and 10 at $0.55 \, \mu m$). It is however difficult to believe that the variations with wavelength of the scattering coefficient and directivity of scattering by (presumably) small grains, may combine in order to produce a substantial wavelength-independent fraction of the total transmitted light. The assumption of large scatterers not included in our calculated optical depths seems more likely. Jura (1994) proposed a

distribution of amorphous carbon spheres close to the MRN one used for the interstellar extinction, in the small radii range. He also added large grains such as the graphitic component found in primitive meteorites (Bernatowicz et al. 1996 and references therein). The balance between absorbed radiation and dust emission could have helped in a spherically symmetric object, which is not the case of IRC+10216 (e.g. Kastner & Weintraub 1994 and references therein). Recent observations shown that, if the red $(0.79\,\mu m)$ or near IR $(1.06\,\mu m)$ images may keep some axial symmetry (Haniff & Buscher 1998), this is definitely not the case of the IR emission, at least during recent years, which comes from five (or possibly seven) resolved bright knots separated by opaque portions (Weigelt et al. 1998, Haniff & Buscher 1998). Skinner et al. (1998) recently obtained HST-WFPC2 images of CW Leo at $(0.83\,\mu m)$. A bright nebula with a dark lane is seen, the authors compare to the one of AFGL2688 (Cygnus Egg Nebula, a bipolar structure). A brighter point like source is however observed in the southern lobe of the CW Leo nebula which is probably the central star. Strong scattering is thus conspicuous.

Images at various short wavelengths would help in setting constraints on the properties of the scattering grains which we believe are large in size. More simultaneous multicolour photometric data has to be obtained before firmer conclusions could be drawn on this fascinating object.

6.7. Discussion of carbon Miras

Fundamentally, carbon-rich Miras and SR or Lb variables populate the same sequence of SEDs. We have found again that Miras exhibit, on the average, larger IR excesses which are interpreted in terms of dust shells with intermediary or large optical optical depths (e.g. Lorenz-Martins & Lefèvre 1993, 1994). What is new is our evaluation of the selective *CS* extinction. We already noted in Sect. 4.2 of Paper I that noticeable curvatures are observed in the IR in part of our dereddening diagrams, while a good linear fit is obtained at shorter wavelengths. It was interpreted as *CS* emission from dust shells of substantial optical depths. For Miras and IRAS C stars, those features practically become the rule. The selective *CS* extinctions found are indicative of small grains (radii $a \leq 0.1\,\mu m$) on the line of sight. Decreasing albedo for single scattering (γ) with increasing wavelength is found for distributions of grains intended to explain the mean interstellar extinction law (see Draine & Lee 1984) we used here. Thus, scattered photons should not yield the agreement observed for the extreme object CW Leo. The albedo for single scattering is not however the whole story since the scattering should be increasingly multiple at shorter wavelengths because of increasing opacity (e.g. Lefèvre et al. 1982, 1983). For a given albedo function $\gamma(\lambda)$, the probability for a scattered photon to finally escape absorption and thus to reach the observer, is increasingly reduced for decreasing wavelengths. This latter opacity effect attenuates the influence of the $\gamma(\lambda)$ (that is what we would observe in an optically thin shell where single scattering predominates at every considered wavelength). There is however no reason why the

Table 6. The seven photometric groups (G) of unreddened carbon variables and the SCV-group of SC stars intermediary between CS and S stars (see Sect. 4). A representative star is mentioned for each group (name in GCVS). Three mean colour indices are given with their standard deviations (see text for details). Replaces Table 1 of Paper I.

G	TYP.S	B-V	CI$_B$	J-K
SCV	UY Cen	2.79 ± 0.10	1.31 ± 0.10	1.44 ± 0.10
CV1	S Cen	1.80 ± 0.33	1.05 ± 0.04	1.42 ± 0.05
CV2	TW Hor	2.39 ± 0.09	1.10 ± 0.06	1.43 ± 0.07
CV3	U Hya	2.62 ± 0.09	1.10 ± 0.06	1.63 ± 0.04
CV4	U Ant	2.95 ± 0.09	1.13 ± 0.07	1.67 ± 0.07
CV5	X Cnc	3.42 ± 0.16	1.11 ± 0.05	1.74 ± 0.06
CV6	RT Cap	4.22 ± 0.18	1.16 ± 0.09	1.97 ± 0.08
CV7	R For	5.23 ± 0.09	1.72 ± 0.03	2.44 ± 0.17

Table 7. A list of the fifty-one carbon variables found unreddened (i.e. with $E(B-V) \leq 0.02$–0.03) in the present study. The stars C-entries in Stephenson (1989) are given; (a): a possible 0.02–0.03 excess is guessed for C833 = R Lep at maximum light (bright epoch); (b): T Cnc is found unreddened at phase 0.1 while *CS* reddening appears at some phases; (c): Miras at maximum light. Replaces Table 2 of Paper I.

CV1	CV2	CV3	CV4	CV5	CV6	CV7
1004	471	1489	234	65	36	361[c]
2331	788	1944	1891	853	833[a]	3652[c]
2635	1264	2244	2685	2077:	1057:	3921[c]
3227	1478	2803	2793	2177	1337	
3558	1881	3374	3368	2378	1877	
	2713	5987		2641	2150	
	2835			3283	2384[b]	
	3665			3313	2877	
	3731			3510	3236	
	5228			3569	3861	
					4774	

spectral energy distribution of scattered photons should follow the CV7-SED attenuated according to the interstellar law we used, i.e. the *transmitted* light. Thus we conclude that, in CW Leo, the contribution of photons scattered to the observer by small (selective) grains $(a \leq 0.1\,\mu m)$ is negligible. Our arguments do not apply to eventual large (non-selective) grains with transmitted and scattered contributions independent of wavelength. We emphasize again that they would escape detection in the present approach. In other words, we only observe direct photons from CW Leo at short wavelengths, unless the possible contribution of large grains $(a \geq 0.3\,\mu m)$ cannot be neglected. If the latter is negligible, the *CS* emission (IR excesses) can be determined from the dereddening diagram. To this purpose, a magnitude difference could be tentatively derived between $y(\lambda)$ from the observations and $y_p(\lambda)$ of Eq. (4) as extrapolated from our model (the straight lines in dereddening diagrams).

Carbon Miras are very few: we were able to find only 73 documented Miras out of nearly 585 carbon stars (687 SEDs) studied so far. Seventeen analyses could not be safely achieved, decreasing the number of well-studied Miras down to 56 stars. It

can be seen in Table 1 that 12 Miras (or possibly so) are classified CV7 at least at some phase, and 7 Miras (or possibly so) can be found in Tables 2 and 3 for CS and SC stars respectively. Unfortunately, many Miras could be studied at only one phase due to missing data. The earliest group reached by some carbon Miras (R Ori and R CMi two CS stars, and Y Per) is HC5 close to their maximum light. The corresponding maximum in effective temperature lies in the 3600–3000 K range.

7. Discussion and conclusion

First of all we summarize our analysis of carbon variables as revised and extended (the CV7 and SCV-groups) in Sects. 3 and 4. Small corrections were operated on the data of Tables 1 and 2 of Paper I to which we substitute Tables 6 and 7. We emphasize again the fact that there is no evidence for gaps between the groups. A continuous classification might be useful later on when a much larger body of data will be available. The reader is referred to Paper I for a full discussion which is not repeated here.

The SCV-group is found intermediary between the carbon stars (CV-groups) and S stars, as discussed in Sect. 4.4. The HC stars were classified into six groups (HC0 to HC5) in Paper II. Some hot carbon-rich related objects were also studied. They can be found either in a HC-group or alternatively in an oxygen-type group. This was the case of part of the RCB variables and of the RV Tau variable AC Her (see Paper II). On the contrary, the carbon stars with IR silicate emission are classified CV1 or CV2 (with the exception of HD 189605 which is HC5, the earlier group just next to CV1), i.e. they exhibit SEDs for carbon variables of early type (see Sect. 5 and Table 4). Finally the carbon and CS Miras can be classified in the above-described scheme, like the SR and Lb variables in Paper I. Many Miras are however very cool objects (CV6 or CV7) with evidences of strong opacities (including *CS* grains whose IR emission is prominent).

While of less accuracy when compared to Paper I studies, the evaluation of the interstellar extinction on HC and SCV stars is quite acceptable (Paper II and Sect. 4.3). Finally, solutions for 585 stars were derived on a homogeneous scale while achieving the studies of 687 carbon SEDs in the three papers. When the SEDs of oxygen-rich stars of Papers II and III are added, this is more than 600 stars analysed so far.

We have been able to disentangle the circumstellar and interstellar extinctions in some cases and large quantities of *CS* grains are inferred from the available data. The comparison between the derived colour excesses and those obtained from maps in the literature proves satisfactory. The difficult point remains the cases of Miras and IRAS C (Sect. 6) including cool CV7 stars (Sect. 3) where extinction and emission from *CS* grains combine with interstellar extinction. The selective *CS* extinction studied at $\lambda \leq 1.25\,\mu\mathrm{m}$ is shown to follow, at least approximately, the law for the diffuse interstellar medium as quoted by Mathis (1990). Scattering from corresponding small grains ($\mathrm{a} \leq 0.1$ or $0.15\,\mu\mathrm{m}$) is shown to have a negligible contribution to the light observed from CW Leo = IRC+10216.

Large carbonaceous scatterers ($\mathrm{a} \geq 0.5\,\mu\mathrm{m}$) are indicated instead. Clearly those extreme objects deserve further studies with additional (preferably simultaneous) data constituting large databases. The authors are aware that many values for Miras in Table 5 are only preliminary.

The next step in our approach will be a calibration of our photometric groups in terms of effective temperatures (Bergeat & Knapik 1999).

References

Alksnis A.K., 1989, Inf. Bull. Var. Stars 3315, 1
Baumert J.H., 1972, unpublished thesis, The Ohio State University
Benson P.J., Little-Marenin I.R., 1987, ApJ 316, L37
Bergeat J., Knapik A., 1997, A&A 321, L9
Bergeat J., Knapik A., 1999, to be submitted to A&A
Bergeat J., Sibille F., Lunel M., 1978, A&A 64, 423
Bergeat J., Knapik A., Rutily B., 1998a, A&A 332, L53
Bergeat J., Knapik A., Rutily B., 1998b, A&A in press (Paper II)
Bernatowicz T.J., Cowsik R., Gibbons P.C., et al., 1996, ApJ 472, 760
Burstein D., Heiles C., 1982, AJ 87, 1165
Catchpole R.M., Feast M.W., 1971, MNRAS 154, 197
Chan S.J., 1994, MNRAS 268, 113
de Jong T., 1989, A&A 223, L23
Doty S.D., Leung C.M., 1998, ApJ 502, 898
Draine B.T., Lee H.M., 1984, ApJ 285, 89
ESA, 1997, The HIPPARCOS Catalogue, ESA SP-1200 (ESA)
FitzGerald M.P., 1968, AJ 73, 983
Gail H.-P., Sedlmayr E., 1988, A&A 206, 153
Glasgold A.E., 1996, ARA&A 34, 241
Gosnell T.R., Hudson H.S., Puetter R.C., 1979, AJ 84, 538
Groenewegen M.A.T., 1997, A&A 317, 503
Haniff C.A., Buscher D.F., 1998, A&A 334, L5
Ivezic Z., Elitzur M., 1995, ApJ 445, 415
IRAS Science Team, 1986, A&AS 65, 607 (LRS)
IRAS Point Source Catalog, version 2, 1988, Joint IRAS Science Working Group, vols. 1–6, NASA RP-1190, U.S. Government Printing Office, Washington D.C.
Jones T.W., Merrill K.M., 1976, ApJ 209, 509
Jorissen A., Mayor M., 1992, A&A 260, 115
Jorissen A., Hennen O., Mayor M., Bruch A., Sterken C., 1985, A&A 301, 707
Jura M., 1994, ApJ 434, 713
Kastner J.H., Weintraub D.A., 1994, ApJ 434, 719
Kazarovets E.V., Samus N.N., 1997, Inf. Bull. Var. Stars 4471, 1. The 73rd name-list of variable stars
Kazarovets E.V., Samus N.N., Goranskij V.P., 1993, Inf. Bull. Var. Stars 3840, 1. The 73rd name-list of variable stars
Keenan P.C., Boeschaar P.C., 1980, ApJS 43, 379
Kholopov P.N., Samus N.N., Frolov M.S., et al., 1985, General Catalogue of Variable Stars. Nauka Publishing House, Moscow (GCVS). Suppl. Lists 67 (1985, IBVS 2681), 68 (1987, IBVS 3058), 69 (1989, IBVS 3323), 70 (1990, IBVS 3530), 71 (1993, IBVS 3840), 72 (1995, IBVS 4140) & 73 (1997, IBVS 4471)
Knapik A., Bergeat J., 1997, A&A 321, 236 (Paper I)
Knapik A., Bergeat J., Rutily B., 1998, A&A 334, 545
Lamy P., 1978, Icarus 34, 68
Le Bertre T., 1987, A&A 176, 107

Le Bertre T., 1988, A&A 203, 85
Le Bertre T., 1992, A&AS 94, 377
Le Bertre T., Gougeon S., Le Sidaner P., 1995, A&AS 299, 791
Lefèvre J., Bergeat J.,, Daniel J.-Y., 1982, A&A 114, 341
Lefèvre J., Daniel J.-Y., Bergeat J., 1983, A&A 121, 51
Little-Marenin I.R., 1986, ApJ 307, L15
Lockwood G.W., 1972, ApJS 24, 375
Lockwood G.W., 1974, ApJ 192, 113
Lockwood G.W., Wing R.F., 1971, ApJ 169, 63
Lorenz-Martins S., Lefèvre J., 1993, A&A 280, 567
Lorenz-Martins S., Lefèvre J., 1994, A&A 291, 831
Lü P.K., 1991, AJ 101, 2229
Mathis J.S., 1990, ARA&A 28, 37
Mattei J.A, 1997, JAAVSO 25, 57
Merrill K.M., Stein W.A., 1976, PASP 88, 294
Noguchi K., Kawara K., Kobayashi Y., et al., 1981, PASJ 33, 373
Neckel T., Klare G., 1980, A&AS 42, 251
Ney E.P., Merrill K.M., 1980, AFGL-TR-80-0050
Pollack J.B., Toon O.B., Khare B.N., 1973, Icarus 19, 372

Rowan-Robinson M., Harris S., 1982, MNRAS 200, 197
Salpeter E.E., 1977, ARA&A 15, 267
Skinner C.J., Griffin I., Whitmore B., 1990, MNRAS 243, 78
Skinner C.J., Meixner M., Bobrowsky M., 1998, MNRAS 300, L29
Sopka R.J., Hildebrand R.H., Jaffe D.T., et al., 1985, ApJ 294, 242
Stephenson C.B., 1973, Pub. of the Warner & Swasey Obs. 1, No. 4
Stephenson C.B., 1976, Pub. of the Warner & Swasey Obs. 2, No. 2
Stephenson C.B., 1989, Pub. of the Warner & Swasey Obs. 3, No. 2
Straniero O., Chieffi A., Limongi M., et al., 1997, ApJ 478, 332
Strecker D.W., Ney E.P., 1974, AJ 79, 797
Wallerstein G., Knapp G.R., 1998, ARA&A 36, 369
Weigelt G., Balega Y., Blöcker T., et al., 1998, A&A 333, L51
Whitelock P.A., Feast M.W., Marang F., Overbeek M.D., 1997, MN-
    RAS 288, 512
Willems F.J., de Jong T., 1986, ApJ 309, L39
Winters J.M., Fleischer A.J., Le Bertre T., Sedlmayr E., 1997, A&A
    326, 305
Zuckerman B., 1993, A&A 276, 367
Zuckerman B., Maddalena R.J., 1989, A&A 223, L20